

THE MONGE-AMPÈRE EQUATION: NOVEL FORMS AND NUMERICAL SOLUTION

V.A. Zheligovsky (vlad@mitp.ru),
O.M. Podvigina

*International Institute of Earthquake Prediction Theory
and Mathematical Geophysics,
84/32 Profsoyuznaya St., Moscow, Russian Federation;*

U. Frisch

*Observatoire de la Côte d'Azur,
U.M.R. 6529, BP 4229, 06304 Nice Cedex 4, France*

Zheligovsky V., Podvigina O., Frisch U. The Monge–Ampère equation:
various forms and numerical methods. *J. Computational Physics*,
229, 2010, 5043-5061 [<http://arxiv.org/abs/0910.1301>]

Monge-Ampère equation: $\det \|u_{x_i, x_j}\| = f(\mathbf{x})$

- **The “2nd order divergence” form**
- **The Fourier integral form**
- **The convolution integral form**
- **A test problem with a cosmological flavour**
- **Numerical solution:**
 - Fixed point algorithm for the regular part of the MAE
 - Algorithm with continuation in a parameter
and discrepancy minimisation
 - Algorithm with improvement of convexity
and discrepancy minimisation
- **Results of solution of the test problem**

Existence and regularity of solutions to the MAE:

- A.V. Pogorelov. The Minkowski multidimensional problem. Nauka, Moscow, 1975. (*Geometric approach, convexity.*)
- I.J. Bakelman. Convex analysis and nonlinear geometric elliptic equations. Springer-Verlag, 1994.
- L.A. Caffarelli, X. Cabré. Fully nonlinear elliptic equations. American Mathematical Society colloquium publications, vol. 43. Amer. Math. Soc., Providence, Rhode Island, 1995. (*The PDE approach, viscous solutions.*)

Methods for discrete optimal transportation problem: ask Andrei Sobolevsky.

Numerical algorithms linked to the geometric interpretation of the MAE:

- V.I. Oliker, L.D. Prussner. On the numerical solution of the equation $\frac{\partial^2 z}{\partial x^2} \frac{\partial^2 z}{\partial y^2} - \left(\frac{\partial^2 z}{\partial x \partial y} \right)^2 = f$ and its discretizations, I. Numerische Mathematik, 54 (1988) 271–293. (*A mesh comprised of 25 points.*)
- D. Michaelis, S. Kudaev, R. Steinkopf, A. Gebhardt, P. Schreiber, A. Bräuer. Incoherent beam shaping with freeform mirror. Nonimaging optics and efficient illumination systems V. Eds. R. Winston, R.J. Koschel. Proc. of SPIE, vol. 7059 (2008) 705905. (*A 55 × 55 mesh, 15 min. of a Pentium 4.*)

Application of algorithms for saddle-point optimisation to the two-dimensional MAE:

- J.-D. Benamou, Y. Brenier. A computational fluid mechanics solution to the Monge–Kantorovich mass transfer problem. *Numerische Mathematik*, 84 (2000) 375–393.
- E.J. Dean, R. Glowinski. Numerical solution of the two-dimensional elliptic Monge–Ampère equation with Dirichlet boundary conditions: an augmented Lagrangian approach. *C. R. Acad. Sci. Paris, Ser. I*, 336 (2003) 779–784.

Various numerical approaches:

- E.J. Dean, R. Glowinski. Numerical solution of the two-dimensional elliptic Monge–Ampère equation with Dirichlet boundary conditions: a least-squares approach. *C. R. Acad. Sci. Paris, Ser. I*, 339 (2004) 887–892.
- E.J. Dean, R. Glowinski. Numerical methods for fully nonlinear elliptic equations of the Monge–Ampère type. *Comput. Methods Appl. Mech. Engrg.* 195 (2006) 1344–1386.
- X. Feng, M. Neilan. Galerkin methods for the fully nonlinear Monge–Ampère equation ([arXiv:0712.1240](https://arxiv.org/abs/0712.1240)).
- X. Feng, M. Neilan. Mixed finite element methods for the fully nonlinear Monge–Ampère equation based on the vanishing moment method ([arXiv:0712.1241](https://arxiv.org/abs/0712.1241)).
- G. Loeper, F. Rapetti. Numerical solution of the Monge–Ampère equation by a Newton’s algorithm. *C. R. Acad. Sci. Paris, Ser. I*, 340 (2005) 319–324. (*A pseudospectral Newton’s algorithm.*)

- J.-D. Benamou, B.D. Froese, A.M. Oberman. Two numerical methods for the elliptic Monge–Ampère equation. Preprint, 2009 [www.divbyzero.ca/froese/w/images/4/40/MA.pdf].

$$u = \nabla^{-2} \sqrt{u_{x_1 x_1}^2 + u_{x_2 x_2}^2 + 2u_{x_1 x_2}^2 + 2f}$$

An iterative Newton–Krylov solver with preconditioning (finite differences, modest accuracy required, discrepancies the order of 10^{-3} – 10^{-4} acceptable):

- G.L. Delzanno, L. Chacón, J.M. Finn, Y. Chung, G. Lapenta. An optimal robust equidistribution method for two-dimensional grid adaptation based on Monge–Kantorovich optimization. *J. Comput. Physics*, 227 (2008) 9841–9864. (256 × 256 grid, contrast ratio= 8886, discrepancy= 7.78×10^{-5} , 70 s. of a 2.4 GHz Intel Xeon processor.)
- J.M. Finn, G.L. Delzanno, L. Chacon. Grid generation and adaptation by Monge–Kantorovich optimization in two and three dimensions. *Proceedings of the 17th International Meshing Roundtable* (2008) 551–568.

The “2nd order divergence” form

A Fourier integral solution in R^N : $u = \int_{R^N} \tilde{u}(\boldsymbol{\omega}) e^{i\boldsymbol{\omega} \cdot \mathbf{x}} d\boldsymbol{\omega}$.

$$\begin{aligned} \det \|a_{ij}\| &\equiv \frac{1}{N!} \sum_{\substack{i_1, \dots, i_N, \\ j_1, \dots, j_N}} \varepsilon_{i_1 \dots i_N} \varepsilon_{j_1 \dots j_N} \prod_{n=1}^N a_{i_n j_n} \quad (\varepsilon_{p_1 \dots p_N} \text{ is the unit antisymmetric tensor of rank } N) \\ \Rightarrow \det \|u_{x_i x_j}\| &= \frac{(-1)^N}{N!} \sum_{\substack{i_1, \dots, i_N, \\ j_1, \dots, j_N}} \varepsilon_{i_1 \dots i_N} \varepsilon_{j_1 \dots j_N} \prod_{n=1}^N \int_{R^N} \tilde{u}(\boldsymbol{\omega}) \omega_{i_n} \omega_{j_n} e^{i\boldsymbol{\omega} \cdot \mathbf{x}} d\boldsymbol{\omega} \\ &= \frac{(-1)^N}{N!} \int_{R^N} \dots \int_{R^N} \left(\sum_{i_1, \dots, i_N} \varepsilon_{i_1 \dots i_N} \prod_{n=1}^N \omega_{i_n}^n \right) \left(\sum_{j_1, \dots, j_N} \varepsilon_{j_1 \dots j_N} \prod_{n=1}^N \omega_{j_n}^n \right) \\ &\quad \times \left(\prod_{n=1}^N \tilde{u}(\boldsymbol{\omega}^n) \right) \exp \left(i \sum_{n=1}^N \boldsymbol{\omega}^n \cdot \mathbf{x} \right) d\boldsymbol{\omega}^1 \dots d\boldsymbol{\omega}^N \\ &= \frac{(-1)^N}{N!} \int_{R^N} \dots \int_{R^N} \det^2 \left\| \boldsymbol{\omega}^1, \dots, \boldsymbol{\omega}^{N-1}, \boldsymbol{\omega} - \sum_{n=1}^{N-1} \boldsymbol{\omega}^n \right\| \\ &\quad \times \left(\prod_{n=1}^{N-1} \tilde{u}(\boldsymbol{\omega}^n) \right) \tilde{u} \left(\boldsymbol{\omega} - \sum_{n=1}^{N-1} \boldsymbol{\omega}^n \right) e^{i\boldsymbol{\omega} \cdot \mathbf{x}} d\boldsymbol{\omega}^1 \dots d\boldsymbol{\omega}^{N-1} d\boldsymbol{\omega} \end{aligned}$$

($\|\boldsymbol{\omega}^1, \dots, \boldsymbol{\omega}^N\|$ is the $N \times N$ matrix comprised of columnar vectors $\boldsymbol{\omega}^1, \dots, \boldsymbol{\omega}^N$)

$$= \frac{(-1)^N}{N!} \int_{R^N} \dots \int_{R^N} \det^2 \|\boldsymbol{\omega}^1, \dots, \boldsymbol{\omega}^{N-1}, \boldsymbol{\omega}\| \left(\prod_{n=1}^{N-1} \tilde{u}(\boldsymbol{\omega}^n) \right) \tilde{u} \left(\boldsymbol{\omega} - \sum_{n=1}^{N-1} \boldsymbol{\omega}^n \right) e^{i\boldsymbol{\omega} \cdot \mathbf{x}} d\boldsymbol{\omega}^1 \dots d\boldsymbol{\omega}^{N-1} d\boldsymbol{\omega}.$$

“Reverse engineering” yields the “second-order divergence” form of the MAE in R^N :

$$\frac{1}{N!} \sum_{i_1, \dots, i_N, j_1, \dots, j_N} \varepsilon_{i_1 \dots i_N} \varepsilon_{j_1 \dots j_N} \left(u_{x_{i_1} x_{j_1}} \dots u_{x_{i_{N-1}} x_{j_{N-1}}} u \right)_{x_{i_N} x_{j_N}} = f.$$

If u is space-periodic, and ϕ is a smooth function with a finite support,

$$\frac{1}{N!} \sum_{\substack{i_1, \dots, i_N, \\ j_1, \dots, j_N}} \varepsilon_{i_1 \dots i_N} \varepsilon_{j_1 \dots j_N} \int_{R^N} u_{x_{i_1} x_{j_1}} \dots u_{x_{i_{N-1}} x_{j_{N-1}}} u \phi_{x_{i_N} x_{j_N}} d\mathbf{x} = \int_{R^3} f \phi d\mathbf{x}.$$

$\forall u \in W_{N-1}^2(T^N)$ the integrals are well-defined

(by the Sobolev embedding theorem, $\nabla u \in L_{2(N-1)}(T^N) \Rightarrow u \in L_\infty(T^N)$).

By contrast, integrals in the similar identity obtained by *one* integration by parts are not well-defined for $u \in W_{N-1}^2(T^N)$.

The Fourier integral form of the MAE

For a space-periodic solution, $0 = \int_{T^3} f \, d\mathbf{x}$.

To accommodate $f > 0$ (of interest in cosmology), let

$$u = \frac{c}{2} |\mathbf{x}|^2 + u', \quad \langle u' \rangle = 0.$$

$\langle \cdot \rangle$ denotes the average: $\langle \mathbf{f} \rangle = \lim_{L \rightarrow \infty} \frac{1}{(2L)^3} \int_{[-L, L]^3} f(\mathbf{x}) \, d\mathbf{x}$.

$$c^N = \langle f \rangle; \quad f/c^N = \int_{R^N} \tilde{f}(\boldsymbol{\omega}) e^{i\boldsymbol{\omega} \cdot \mathbf{x}} \, d\boldsymbol{\omega}.$$

$$\begin{aligned} \nabla^2 u' &= \int_{R^N} \tilde{\varphi}(\boldsymbol{\omega}) e^{i\boldsymbol{\omega} \cdot \mathbf{x}} \, d\boldsymbol{\omega}, & u' &= \int_{R^N} \tilde{u}'(\boldsymbol{\omega}) e^{i\boldsymbol{\omega} \cdot \mathbf{x}} \, d\boldsymbol{\omega} \\ \Rightarrow \tilde{u}'(\boldsymbol{\omega}) &= -\tilde{\varphi}(\boldsymbol{\omega}) / |\boldsymbol{\omega}|^2. \end{aligned}$$

$$\det \|u'_{x_i x_j}\| = \frac{1}{N!} \int_{R^N} \cdots \int_{R^N} \det^2 \left\| \mathbf{i}_{\boldsymbol{\omega}^1}, \dots, \mathbf{i}_{\boldsymbol{\omega}^{N-1}}, \mathbf{i}_{\boldsymbol{\omega} - \sum_{n=1}^{N-1} \boldsymbol{\omega}^n} \right\| \\ \times \left(\prod_{n=1}^{N-1} \tilde{\varphi}(\boldsymbol{\omega}^n) \right) \tilde{\varphi} \left(\boldsymbol{\omega} - \sum_{n=1}^{N-1} \boldsymbol{\omega}^n \right) e^{i\boldsymbol{\omega} \cdot \mathbf{x}} d\boldsymbol{\omega}^1 \dots d\boldsymbol{\omega}^{N-1} d\boldsymbol{\omega}$$

($\mathbf{i}_{\mathbf{a}}$ is a unit vector in the direction of \mathbf{a}). Consider the term of order $m < N$ in u' :

$$\frac{(-1)^m}{N!} \sum_{i_1, \dots, i_N, j_1, \dots, j_N} \varepsilon_{i_1 \dots i_N} \varepsilon_{j_1 \dots j_N} \sum_{|\sigma|=m} \left(\prod_{n: i_n, j_n \in \sigma} \int_{R^N} \tilde{u}'(\boldsymbol{\omega}) \omega_{i_n} \omega_{j_n} e^{i\boldsymbol{\omega} \cdot \mathbf{x}} d\boldsymbol{\omega} \right) \prod_{n: i_n \text{ or } j_n \notin \sigma} \delta_{i_n j_n}$$

(the sum $\sum_{|\sigma|=m}$ is over all subsets $\sigma \subset \{1, \dots, N\}$ of cardinality m ; $\delta_{i_n j_n}$ is the Kronecker symbol)

$$= \frac{(-1)^m}{m!} \sum_{1 \leq p_1 < \dots < p_{N-m} \leq N} \int_{R^N} \cdots \int_{R^N} \left(\sum_{j_1, \dots, j_m} \varepsilon_{j_1 \dots j_m p_1 \dots p_{N-m}} \prod_{n=1}^m \omega_{j_n}^n \right)^2 \\ \times \left(\prod_{n=1}^m \tilde{u}'(\boldsymbol{\omega}^n) \right) \exp \left(i \sum_{n=1}^m \boldsymbol{\omega}^n \cdot \mathbf{x} \right) d\boldsymbol{\omega}^1 \dots d\boldsymbol{\omega}^m \\ = \int_{R^N} \cdots \int_{R^N} A_m \left(\mathbf{i}_{\boldsymbol{\omega}^1}, \dots, \mathbf{i}_{\boldsymbol{\omega}^{m-1}}, \mathbf{i}_{\boldsymbol{\omega} - \sum_{n=1}^{m-1} \boldsymbol{\omega}^n} \right) \\ \times \left(\prod_{n=1}^{m-1} \tilde{\varphi}(\boldsymbol{\omega}^n) \right) \tilde{\varphi} \left(\boldsymbol{\omega} - \sum_{n=1}^{m-1} \boldsymbol{\omega}^n \right) e^{i\boldsymbol{\omega} \cdot \mathbf{x}} d\boldsymbol{\omega}^1 \dots d\boldsymbol{\omega}^{m-1} d\boldsymbol{\omega},$$

where $A_m(\mathbf{i}^1, \dots, \mathbf{i}^m) \equiv \frac{1}{m!} \sum_{1 \leq p_1 < \dots < p_{N-m} \leq N} M_{p_1 \dots p_{N-m}}^2(\mathbf{i}^1, \dots, \mathbf{i}^m)$

is the sum of squares of all minors of rank m ,

$$M_{p_1 \dots p_{N-m}}(\mathbf{i}^1, \dots, \mathbf{i}^m) \equiv \sum_{j_1, \dots, j_m} \varepsilon_{j_1 \dots j_m p_1 \dots p_{N-m}}(\mathbf{i}^1)_{j_1} \dots (\mathbf{i}^m)_{j_m},$$

obtained by crossing out rows of numbers $p_1 < \dots < p_{N-m}$ from the $N \times m$ matrix

$$\mathcal{M}_m \equiv \|\mathbf{i}^1, \dots, \mathbf{i}^m\|,$$

comprised of m columnar vectors $\mathbf{i}^1, \dots, \mathbf{i}^m$.

The Fourier integral form of the MAE:

$$\begin{aligned} & \tilde{\varphi}(\boldsymbol{\omega}) + \sum_{m=2}^N \int_{R^N} \dots \int_{R^N} A_m(\mathbf{i}\boldsymbol{\omega}^1, \dots, \mathbf{i}\boldsymbol{\omega}^{m-1}, \mathbf{i}\boldsymbol{\omega}_{-\sum_{n=1}^{m-1}} \boldsymbol{\omega}^n) \\ & \times \left(\prod_{n=1}^{m-1} \tilde{\varphi}(\boldsymbol{\omega}^n) \right) \tilde{\varphi}\left(\boldsymbol{\omega} - \sum_{n=1}^{m-1} \boldsymbol{\omega}^n\right) d\boldsymbol{\omega}^1 \dots d\boldsymbol{\omega}^{m-1} = \tilde{f}(\boldsymbol{\omega}), \quad \forall \boldsymbol{\omega} \neq 0. \end{aligned}$$

Sharp bounds for the kernels A_m in the Fourier integral form:

$$0 \leq A_m(\mathbf{i}^1, \dots, \mathbf{i}^m) \leq \frac{1}{m!}$$

By the Gram–Schmidt orthogonalisation process, change $\mathbf{i}^s \rightarrow \mathbf{j}^s$ such that

(i) $\mathbf{j}^1 = \mathbf{i}^1$,

(ii) $\forall s$, \mathbf{j}^s differs from \mathbf{i}^s by a linear combination of $\mathbf{i}^{s'}$ for $s' < s$ ($\Rightarrow A_m$ is unaltered),

(iii) $\forall s$, \mathbf{j}^s is orthogonal to all $\mathbf{j}^{s'}$ for $s' < s$

$\Rightarrow |\mathbf{j}^s| = \sin \theta_s$, where θ_s is the angle between \mathbf{i}^s and the subspace spanned by $\{\mathbf{i}^{s'} \mid s' < s\}$.

Denote $\mathbf{v}^s = \mathbf{i}_{\mathbf{j}^s}$.

$$\Rightarrow A_m(\mathbf{i}^1, \dots, \mathbf{i}^m) = A_m(\mathbf{v}^1, \dots, \mathbf{v}^m) \prod_{s=2}^m \sin^2 \theta_s$$

Denote $\mathcal{M}'_m \equiv \|\mathbf{v}^1, \dots, \mathbf{v}^m\|$ and ${}^t\mathcal{M}'_m$ the transpose of \mathcal{M}'_m .

$$\det \|a_{ij}\| = \sum_{j_1, \dots, j_m} \varepsilon_{j_1 \dots j_m} \prod_{i=1}^m a_{ij_i} \Rightarrow \sum_{1 \leq p_1 < \dots < p_{N-m} \leq N} M_{p_1 \dots p_{N-m}}^2(\mathbf{v}^1, \dots, \mathbf{v}^m) = \det({}^t\mathcal{M}'_m \mathcal{M}'_m)$$

(the orthogonality of $\{\mathbf{v}^1, \dots, \mathbf{v}^m\}$ is not required).

Enlarge the set $\{\mathbf{v}^1, \dots, \mathbf{v}^m\}$ by vectors \mathbf{v}^s for $s > m$ to a complete orthonormal basis in R^N
 $\Rightarrow \mathcal{V} = \|\mathbf{v}^1, \dots, \mathbf{v}^N\|$ is an orthogonal matrix.

Let \mathcal{E} be an $N \times m$ matrix, such that $\mathcal{E}_{ps} = 0$ except for $\mathcal{E}_{ss} = 1 \forall s, 1 \leq s \leq m$.

$$\Rightarrow \mathcal{M}'_m = \mathcal{V}\mathcal{E},$$

$$\Rightarrow \det({}^t\mathcal{M}'_m\mathcal{M}'_m) = \det({}^t\mathcal{E}^t\mathcal{V}\mathcal{V}\mathcal{E}) = \det({}^t\mathcal{E}\mathcal{E}) = \det\mathcal{I}_m = 1$$

(\mathcal{I}_m is the identity matrix of size m).

$$\Rightarrow A_m(\mathbf{i}^1, \dots, \mathbf{i}^m) = \frac{1}{m!} \prod_{s=2}^m \sin^2 \theta_s.$$

QED.

Solution of the MAE for a weakly fluctuating r.h.s.

If $f - \langle f \rangle$ is small (relative the mean $\langle f \rangle$), then $\tilde{\varphi}(\boldsymbol{\omega}) \approx \tilde{f}(\boldsymbol{\omega})$.

$$\begin{aligned} \tilde{\varphi}_{K+1}(\boldsymbol{\omega}) &= \tilde{f}(\boldsymbol{\omega}) - \sum_{m=2}^N \int_{R^N} \dots \int_{R^N} A_m \left(\mathbf{i}_{\boldsymbol{\omega}^1}, \dots, \mathbf{i}_{\boldsymbol{\omega}^{m-1}}, \mathbf{i}_{\boldsymbol{\omega} - \sum_{n=1}^{m-1} \boldsymbol{\omega}^n} \right) \\ &\quad \times \left(\prod_{n=1}^{m-1} \tilde{\varphi}_K(\boldsymbol{\omega}^n) \right) \tilde{\varphi}_K \left(\boldsymbol{\omega} - \sum_{n=1}^{m-1} \boldsymbol{\omega}^n \right) d\boldsymbol{\omega}^1 \dots d\boldsymbol{\omega}^{m-1}. \end{aligned}$$

Theorem

1°. *Suppose*

$$C_0 > 0, \quad C_1 > 0, \quad \sum_{m=2}^N \frac{(C_0 + C_1)^m}{m!} \leq C_1, \quad \int_{R^N} |\tilde{f}(\boldsymbol{\omega})| d\boldsymbol{\omega} \leq C_0,$$

and for $K = 0$

$$\int_{R^N} |\tilde{\varphi}_K(\boldsymbol{\omega}) - \tilde{f}(\boldsymbol{\omega})| d\boldsymbol{\omega} \leq C_1. \quad (*)$$

Then (*) holds true $\forall K > 0$.

2°. Under the same conditions,

$$\int_{R^N} |\tilde{\varphi}_{K+1}(\boldsymbol{\omega}) - \tilde{\varphi}_K(\boldsymbol{\omega})| d\boldsymbol{\omega} \leq C_2 \int_{R^N} |\tilde{\varphi}_K(\boldsymbol{\omega}) - \tilde{\varphi}_{K-1}(\boldsymbol{\omega})| d\boldsymbol{\omega},$$

$$\max_{\boldsymbol{\omega} \in R^N} |\tilde{\varphi}_{K+1}(\boldsymbol{\omega}) - \tilde{\varphi}_K(\boldsymbol{\omega})| \leq C_2 \max_{\boldsymbol{\omega} \in R^N} |\tilde{\varphi}_K(\boldsymbol{\omega}) - \tilde{\varphi}_{K-1}(\boldsymbol{\omega})|,$$

hold true $\forall K > 0$, where

$$C_2 \equiv \sum_{m=1}^{N-1} \frac{(C_0 + C_1)^m}{m!}.$$

If $C_2 < 1$, the iterations converge to a solution, unique in the ball

$$\int_{R^N} |\tilde{\varphi}(\boldsymbol{\omega}) - \tilde{f}(\boldsymbol{\omega})| d\boldsymbol{\omega} \leq C_1.$$

For $N = 3$, $C_0 = \sqrt{3} - 4/3$, $C_1 = 1/3$.

Note that $C_0 < 1$ and hence $\int_{R^N} |\tilde{f}(\boldsymbol{\omega})| d\boldsymbol{\omega} \leq C_0$ implies $f > 0$ everywhere.

Note that the domain of the solution is non-compact (the entire R^N).

The “convolution” form of the MAE

Set

$$\tilde{\xi}(\boldsymbol{\omega}) \equiv \sqrt{\tilde{u}(\boldsymbol{\omega})/(2\pi)^N} \quad (\tilde{\xi}(0) = 0),$$

$$\arg(\tilde{\xi}(\boldsymbol{\omega})) = \arg(\tilde{u}'(\boldsymbol{\omega}))/2, \quad \text{if } |\arg(\tilde{u}'(\boldsymbol{\omega}))| < \pi;$$

$$\arg(\tilde{\xi}(\boldsymbol{\omega})) = -\arg(\tilde{\xi}(-\boldsymbol{\omega})), \quad \text{if } \arg(\tilde{u}'(\boldsymbol{\omega})) = \pi.$$

$$\Rightarrow \xi(\mathbf{x}) \equiv \int_{R^N} \tilde{\xi}(\boldsymbol{\omega}) e^{i\boldsymbol{\omega} \cdot \mathbf{x}} d\boldsymbol{\omega} \text{ is a real-valued function (not uniquely defined).}$$

Consider the term of order m in u' (note $\int_{R^N} e^{i\boldsymbol{\omega} \cdot \mathbf{x}} d\boldsymbol{\omega} = (2\pi)^N \delta(\mathbf{x})$):

$$\begin{aligned} & (-1)^m \int_{R^N} \cdots \int_{R^N} A_m(\boldsymbol{\omega}^1, \dots, \boldsymbol{\omega}^m) \left(\prod_{n=1}^m \tilde{u}'(\boldsymbol{\omega}^n) \right) \exp\left(i \sum_{n=1}^m \boldsymbol{\omega}^n \cdot \mathbf{x}\right) d\boldsymbol{\omega}^1 \dots d\boldsymbol{\omega}^m \\ &= \left(- (2\pi)^N\right)^m \int_{R^N} \cdots \int_{R^N} A_m(\tilde{\xi}(\boldsymbol{\omega}^1)\boldsymbol{\omega}^1, \dots, \tilde{\xi}(\boldsymbol{\omega}^m)\boldsymbol{\omega}^m) \exp\left(i \sum_{n=1}^m \boldsymbol{\omega}^n \cdot \mathbf{x}\right) d\boldsymbol{\omega}^1 \dots d\boldsymbol{\omega}^m \\ &= (2\pi)^{-Nm} \int_{R^N} \cdots \int_{R^N} A_m \left(\int_{R^N} \nabla \xi(\mathbf{x}) e^{-i\boldsymbol{\omega}^1 \cdot \mathbf{x}^1} d\mathbf{x}^1, \dots, \int_{R^N} \nabla \xi(\mathbf{x}) e^{-i\boldsymbol{\omega}^m \cdot \mathbf{x}^m} d\mathbf{x}^m \right) \\ & \quad \times \exp\left(i \sum_{n=1}^m \boldsymbol{\omega}^n \cdot \mathbf{x}\right) d\boldsymbol{\omega}^1 \dots d\boldsymbol{\omega}^m \\ &= \frac{1}{m!} \int_{R^N} \cdots \int_{R^N} \det \left({}^t \|\nabla \xi(\mathbf{x}^1), \dots, \nabla \xi(\mathbf{x}^m)\| \|\nabla \xi(\mathbf{x} - \mathbf{x}^1), \dots, \nabla \xi(\mathbf{x} - \mathbf{x}^m)\| \right) d\mathbf{x}^1 \dots d\mathbf{x}^m. \end{aligned}$$

The “*convolution*” form of the MAE:

$$1 + \sum_{m=1}^N \frac{1}{m!} \int_{R^N} \dots \int_{R^N} \det \left({}^t \|\nabla \xi(\mathbf{x}^1), \dots, \nabla \xi(\mathbf{x}^m)\| \right. \\ \left. \times \|\nabla \xi(\mathbf{x} - \mathbf{x}^1), \dots, \nabla \xi(\mathbf{x} - \mathbf{x}^m)\| \right) d\mathbf{x}^1 \dots d\mathbf{x}^m = f/c^N.$$

A test problem with a cosmological flavour

The reconstruction of the dynamical history of the Universe from present observations of the spatial distribution of masses:

- The distribution of masses at the epoch of matter-radiation decoupling ($\sim 380\,000$ years after the Big Bang) is uniform.
- For the dynamics of matter on sufficiently large scales (of the order of a few million light years) the Lagrangian map from initial to current mass locations is approximately the gradient of a convex potential. This holds exactly for the Zel’dovich approximation and for its refinement, the first-order Lagrangian perturbation approximation.
- The potential of the map satisfies the MAE, whose r.h.s. is the (known) ratio of densities at the present and initial positions.
- The r.h.s. being positive, the solution is a convex function.

★ We solve the MAE for $N = 3$ and a mass distribution for G “localised objects” (δ is small):

$$f = \delta^{-3} \sum_{g=1}^G f^{(g)} \left(\frac{\mathbf{r} - \mathbf{r}^{(g)}}{\delta} \right).$$

★ The g -th “object” of mass $m^{(g)} > 0$ is located at $\mathbf{r}^{(g)}$ and has a Gaussian density distribution:

$$f^{(g)}(\mathbf{r}) = \frac{m^{(g)}}{(\sigma^{(g)}\sqrt{\pi})^3} \exp(-|\mathbf{r}/\sigma^{(g)}|^2).$$

★ We seek a solution $u = \frac{c}{2}|\mathbf{x}|^2 + u'$ with a space-periodic zero-mean u' , assuming that the space-periodic r.h.s. \hat{f} of the MAE is the sum of “clones” of $f^{(g)}$ over all periodicity cells.

★ The total mass is normalised:

$$\int f(\mathbf{r}) d\mathbf{r} = \sum_{g=1}^G m^{(g)} = 1 \quad \Rightarrow \quad c = 1.$$

An exact solution to the MAE for a spherically symmetric mass distribution

In spherical coordinates centred at $\mathbf{r}^{(g)}$, for spherically symmetric u and f , the MAE is

$$\rho^{-2} \frac{\partial^2 u}{\partial \rho^2} \left(\frac{\partial u}{\partial \rho} \right)^2 = \delta^{-3} f,$$

where $\rho = |\mathbf{r} - \mathbf{r}^{(g)}|$. A solution,

$$u(\rho, \delta) = \int_0^\rho \left(3 \int_0^{r'/\delta} r^2 f(r) dr \right)^{1/3} dr',$$

has uniformly bounded first derivatives:

$$\frac{\partial u}{\partial x_i} = \frac{x_i}{\rho} \left(3 \int_0^{\rho/\delta} r^2 f(r) dr \right)^{1/3} = O(\delta^0)$$

and $O(\delta^{-1})$ second derivatives:

$$\frac{\partial^2 u}{\partial x_i \partial x_m} = \delta^{-1} \frac{x_i x_m}{\rho^2} \left(\frac{\rho}{\delta} \right)^2 f \left(\frac{\rho}{\delta} \right) \left(3 \int_0^{\rho/\delta} r^2 f(r) dr \right)^{-2/3} + \left(\delta_m^i - \frac{x_i x_m}{\rho^2} \right) \frac{1}{\rho} \left(3 \int_0^{\rho/\delta} r^2 f(r) dr \right)^{1/3},$$

since

- $|x_i x_m / \rho^2| \leq 1$;
- for $\rho < \delta$, $f(\rho/\delta)$ is uniformly bounded and

$$\underline{c}(\rho/\delta)^3 \leq \int_0^{\rho/\delta} r^2 f(r) dr \leq \bar{c}(\rho/\delta)^3$$

for some positive constant \underline{c} and \bar{c} ;

- for $\rho \geq \delta$, $(\rho/\delta)^2 f(\rho/\delta)$ is uniformly bounded and

$$0 < \underline{c}' \leq \int_0^{\rho/\delta} r^2 f(r) dr \leq \bar{c}'$$

for some constant \underline{c}' and \bar{c}' .

Moreover, if ρ is larger than a positive constant, $f(\rho/\delta) = o(\delta^3)$,

\Rightarrow all second derivatives of u are uniformly bounded outside any sphere of a fixed radius.

A one-cell solution to the MAE for $G > 1$ spherically symmetric localised objects

A solution for $G > 1$ objects can be expected to admit a power series expansion

$$u(\mathbf{r}) = \sum_{n=0} u_n(\mathbf{r}, \delta) \delta^n, \quad (*)$$

where $\forall n$ (by analogy with the one-object solution) $u_n(\mathbf{r}, \delta) = O(\delta^0)$ and $|\nabla u_n(\mathbf{r}, \delta)| = O(\delta^0)$. We can expect interaction of one-object solutions $u^{(g)}(|\mathbf{r} - \mathbf{r}^{(g)}|, \delta)$ to be asymptotically unimportant:

$$u_0(\mathbf{r}) = \sum_{g=0} u^{(g)}(|\mathbf{r} - \mathbf{r}^{(g)}|, \delta).$$

Consider a neighbourhood of an object γ . In the leading order, the l.h.s. of the MAE is $\det \|u_{0\ x_i x_j}\|$. For $g \neq \gamma$, $|u_{x_i x_j}^{(g)}| = O(\delta^0) \Rightarrow$ only triple products of $u_{x_i x_j}^{(\gamma)}$ contribute in the leading order, $O(\delta^{-3})$; they do match the l.h.s. (Nonlinear interaction of pairs of one-object solutions is $O(\delta^{-2})$, and that of triplets $O(\delta^{-1})$.)

Nevertheless, (*) is NOT the leading order term: it is $O(|\mathbf{r}|)$ for $|\mathbf{r}| \rightarrow \infty$, and not $O(|\mathbf{r}|^2)$. Furthermore, we cannot construct a global periodic solution summing up the periodically distributed “clones” of one-cell solutions (*) – the sum is infinite; there would be infinitely many pairwise interactions between objects yielding products of the order $O(\delta^{-2})$, and the pairwise interaction does not become weaker when the distance between the interacting objects grows.

Numerical solution of the odd-dimensional MAE

A basic solver, FPAR

An observation: If the kernels A_m in the Fourier integral form

$$\begin{aligned} & \tilde{\varphi}(\boldsymbol{\omega}) + \sum_{m=2}^N \int_{R^N} \dots \int_{R^N} A_m \left(\mathbf{i}\boldsymbol{\omega}^1, \dots, \mathbf{i}\boldsymbol{\omega}^{m-1}, \mathbf{i}\boldsymbol{\omega} - \sum_{n=1}^{m-1} \boldsymbol{\omega}^n \right) \\ & \times \left(\prod_{n=1}^{m-1} \tilde{\varphi}(\boldsymbol{\omega}^n) \right) \tilde{\varphi} \left(\boldsymbol{\omega} - \sum_{n=1}^{m-1} \boldsymbol{\omega}^n \right) d\boldsymbol{\omega}^1 \dots d\boldsymbol{\omega}^{m-1} = \tilde{f}(\boldsymbol{\omega}), \quad \forall \boldsymbol{\omega} \neq 0 \end{aligned}$$

are frozen: $A_m = a_m$, the new system of equations is just the Fourier form of the equation

$$\sum_{m=1}^N a_m \eta^m = f / \langle f \rangle$$

in the physical space.

The Fixed Point Algorithm for the Regular part of the MAE:

For $\eta = \nabla^2 u'$, transform the MAE: $\sum_{m=1}^N a_m \eta^m = f / \langle f \rangle + F(\eta)$,

where $F(\eta) \equiv \sum_{m=1}^N a_m \eta^m - \det \|\nabla^{-2}(\eta_{x_i x_j}) + \delta_{ij}\|$.

Iterate in the physical space: $\sum_{m=1}^N a_m \eta_K^m = f / \langle f \rangle + F(\eta_{K-1})$.

$0 \leq A_m \leq 1/m!$ for $m > 0 \Rightarrow$ it is practical to set $a_1 = 1$; $a_m = 1/(2m!)$ for $m > 1$.

For $a_1 = 1$, the linear in u' term is treated exactly,

$$F(\eta) = \sum_{m=2}^N \int_{R^N} \dots \int_{R^N} (A_m(\mathbf{i}\boldsymbol{\omega}^1, \dots, \mathbf{i}\boldsymbol{\omega}^m) - a_m) \left(\prod_{n=1}^m \tilde{\varphi}(\boldsymbol{\omega}^n) \right) \exp\left(i \sum_{n=1}^m \boldsymbol{\omega}^n \cdot \mathbf{x}\right) d\boldsymbol{\omega}^1 \dots d\boldsymbol{\omega}^m - 1,$$

and for $m \geq 2$, for our a_m , $|A_m(\mathbf{i}\boldsymbol{\omega}^1, \dots, \mathbf{i}\boldsymbol{\omega}^m) - a_m| \leq a_m$.

The l.h.s. ‘‘captures’’ the nonlinear behaviour of the l.h.s. of the MAE, and the algorithm has chances to converge. Since $|A_m - a_m| = a_m$ for the extreme values of A_m , convergence is not guaranteed.

Lemma. \forall odd N and the chosen a_m ,

$$P_N(\eta) \equiv \sum_{m=1}^N a_m \eta^m = \ell$$

has a unique root for any r.h.s.

Proof.

$$P'_N(\eta) - P''_N(\eta) = \frac{1}{2} \left(1 + \frac{\eta^{N-1}}{(N-1)!} \right).$$

At a minimum of $P'_N(\eta)$, $P''_N(\eta) = 0 \Rightarrow P'_N > 0$ identically. QED.

(Similarly, \forall even N the number of roots of P_N is 0 or 2.)

In an application to a test problem inspired by cosmology produces a sequence of iterations, initially converging, but subsequently blowing up.

A more advanced solver, ACPDM

(Algorithm with Continuation in a Parameter and Discrepancy Minimisation)

I. Continuation in the parameter $p \in [0, 1]$:

A generalisation of the MAE: $Q(\eta; p) \equiv \sum_{m=1}^N a_m \eta^m - f/\langle f \rangle - pF(\eta) = 0$, (*)

For $p = 0$, this is a set of polynomial equations of degree N ; for $p = 1$ this is the MAE. Solve (*) for some p_j increasing from 0 to 1, with application of the FPAR iterations

$$\sum_{m=1}^N a_m \eta_K^m = f/\langle f \rangle + pF(\eta_{K-1}).$$

Obtain an initial approximation of the solution for $p = p_j$ by polynomial extrapolation over all nodes $p_{j'} < p_j$ (use quadruple precision).

We monitor the r.m.s. discrepancy $d(\eta, p) \equiv \sqrt{\langle (Q(\eta; p) - \langle Q(\eta; p) \rangle)^2 \rangle}$.

(Note $\langle Q(\eta; 1) \rangle = 0 \Rightarrow d(\eta, 1) \equiv \sqrt{\langle (\det \|\nabla^{-2} \eta_{x_i x_j} + \delta_{ij}\| - f/\langle f \rangle)^2 \rangle}$.)

II. Minimisation of the residual in Krylov spaces:

(The idea is borrowed from, e.g., GMRES; actually we employ a pJFNK without N.)

If η' and η'' are approximate solutions to the gMAE, $Q(\eta; p) = 0$, then

$$Q(\eta'; p) - Q(\eta''; p) = J(\eta' - \eta'') + O(\|\eta' - \eta''\|^2),$$

where J is the operator of linearisation of the gMAE around the solution.

Let (\cdot, \cdot) denote a scalar product, e.g., of the Lebesgue space $L^2(T^3)$: $(\mathbf{u}, \mathbf{v}) = \int_{T^3} u(\mathbf{x})v(\mathbf{x})d\mathbf{x}$ and $\|\cdot\|$ the induced norm of a scalar field: $\|\mathbf{v}\| \equiv \sqrt{(\mathbf{v}, \mathbf{v})}$.

ACPDM proceeds by **sequences of stabilised iterations**. ($f > 0$ is not required.)

To make an iteration, an approximate solution η_K , and two sets of S scalar fields, $v_s(\mathbf{x})$ and $w_s(\mathbf{x})$, $0 \leq s \leq S$, where $0 \leq S \leq S_{\max}$ (in our runs, $S_{\max} = 5$), are required.

All v_s are mutually (\cdot, \cdot) -orthogonal, and $v_s = Jw_s + O(\|w_s\|^2)$ for small w_s .

A *sequence of stabilised iterations of ACPDM* is initialised using the current approximation η_0 for computation of an FPAR iteration $\eta_1 = \eta'_1$, and setting $S = 0$.

For $K > 1$, a stabilised iteration of ACPDM consists of 6 steps:

i. Make an FPAR iteration, i.e., at each grid point in the physical space solve

$$\sum_{m=1}^N a_m (\eta'_K)^m = f / \langle f \rangle + pF(\eta_K).$$

ii. Compute the discrepancy field $Q(\eta'_K)$.

iii. Orthogonalise $v' \equiv Q(\eta'_K) - Q(\eta'_{K-1})$ to all v_s , $1 \leq s \leq S$, and set

$$v_{S+1} = v' - \sum_{s=1}^S \frac{(v', v_s)}{(v_s, v_s)} v_s, \quad w_{S+1} = \eta'_K - \eta'_{K-1} - \sum_{s=1}^S \frac{(v', v_s)}{(v_s, v_s)} w_s.$$

iv. Minimise the discrepancy $\|Q(\eta'_K - \sum_{s=1}^S q_s w_s)\|$, setting

$$\eta_{K+1} = \eta'_K - \sum_{s=1}^{S+1} \frac{(Q(\eta'_K), v_s)}{(v_s, v_s)} w_s.$$

v. If $S < S_{\max}$, increase S by 1; otherwise (i.e., if $S = S_{\max}$), discard v_1 and w_1 , and decrease by 1 the indices s of the remaining S_{\max} fields v_s and w_s .

vi. Compute the r.h.s. of the equation defining the iterations for η'_{K+1} , $Q(\eta_{K+1})$, and $d(\eta_{K+1})$. If $d(\eta_{K+1}) < \varepsilon$, then η_{K+1} is the approximate solution for the present p .

If $\|Q(\eta_{K+1})\| > \|Q(\eta_K)\|$, the current sequence is terminated (the effect of the nonlinearity is significant; need small S_{\max}).

Summary.

- ACPDM performs continuation in the parameter p .
- For a given p , start by carrying out the FPAR iterations.
- When the convergence slows down (in our runs $d^2(\eta_K) > d^2(\eta_{K-1})/2$), start a sequence of stabilised iterations.
- If the sequence terminates in step vi , make the FPAR iterations while $d^2(\eta_K) > \alpha d^2(\eta_{K-1})$; upon termination, start a new sequence. (α can slightly exceed 1 in order to allow the transients to die off and the dominant instability modes to set in; we employed $\alpha = 1.05$).

Application to a test problem inspired by cosmology

A poor man's Universe: $G = 3$ galaxies in the periodicity cell T^3 , $-1/2 \leq x_i \leq 1/2$:

$$m^{(1)} : m^{(2)} : m^{(3)} = \frac{1}{18} : \frac{1}{27} : \frac{1}{32},$$

$$\delta = 1, \quad \sigma^{(1)} = \sigma^{(2)} = \frac{1}{6}, \quad \sigma^{(3)} = \frac{1}{8},$$

$$\mathbf{r}^{(1)} = \frac{1}{4}(-1, 1, -1), \quad \mathbf{r}^{(2)} = \frac{1}{4}(1, -1, -1), \quad \mathbf{r}^{(3)} = \frac{1}{4}(-1, -1, 1).$$

- The r.h.s. achieves its maximum at $\mathbf{r}^{(3)}$ and the minimum at $\frac{1}{4}(1, 1, 1)$;
- The contrast number is $\approx 1.313 \times 10^7$.
- A uniform grid is comprised of 64^3 points in the periodicity cell T^3 .
- $\det \|u'_{x_i x_j} + \delta_{ij}\|$ is computed by the pseudospectral method with dealiasing (for $N = 3$ this requires to compute $u'_{x_i x_j}$ in the physical space on the grid of 128^3 points).
- The fall off of the energy spectrum of $\eta = \nabla^2 u'$ is fast (11 orders of magnitude).

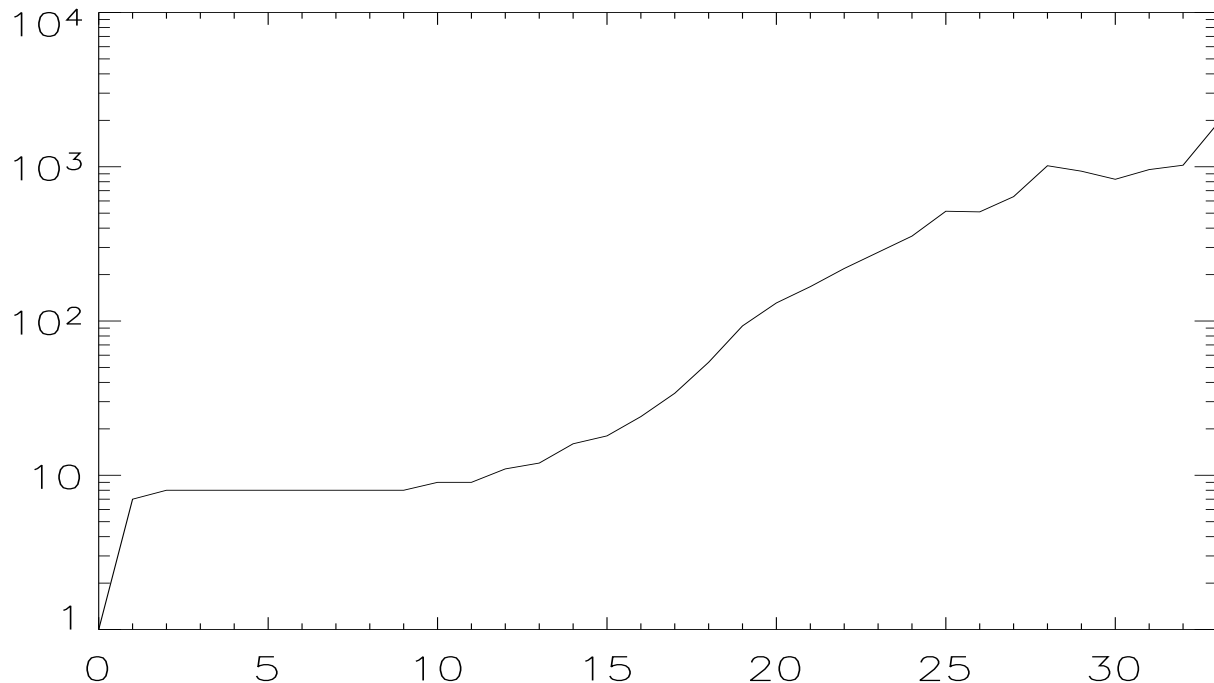
- ★ When applied for $J = 20$ nodes $p_j = j/J$, $j = 0, \dots, J - 1$, convergence of ACPDM is fast.
- ★ A polynomial 20-node extrapolation yields an approximate solution with the accuracy $d(\eta, 1) = 0.47 \times 10^{-2}$ and $d_\infty(\eta, 1) = 0.02$, where

$$d_\infty(\eta, 1) \equiv \max_{T^3} \left| \det \|u'_{x_i x_j} + \delta_{ij}\| - \hat{f}/\langle \hat{f} \rangle \right|.$$

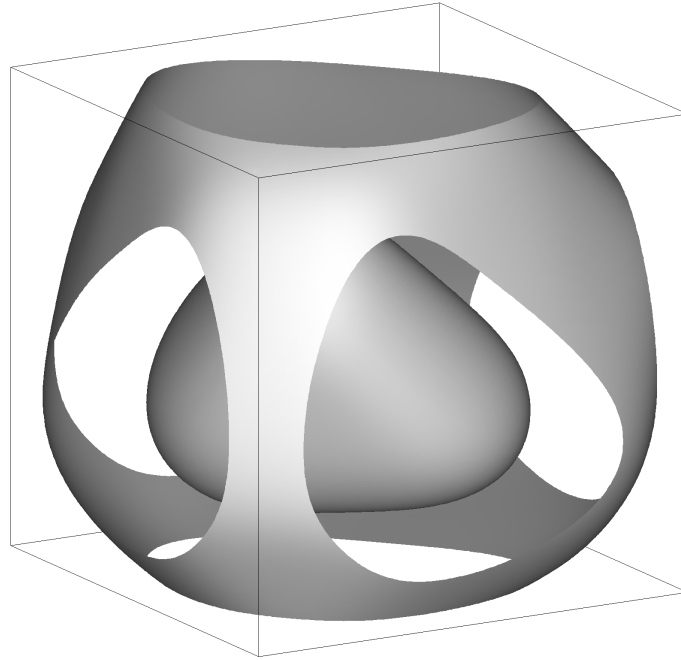
- ★ When it is used as an initial approximation for a run for $p = 1$, the pattern of convergence is erratic; after 38 685 evaluations of the determinant of the Hessian, $d(\eta, 1) = 0.99 \times 10^{-9}$ and $d_\infty(\eta, 1) = 0.39 \times 10^{-7}$, and convergence stalls.
- ★ ACPDM ceases to stall, after $J' = 13$ nodes are added to the mesh:

$$p_j = j/J, \quad j = 0, \dots, J - 1; \quad p_{J+j-1} = 1 - (2^j J)^{-1}, \quad j = 1, \dots, J'.$$

- ★ A polynomial extrapolation over the 33 nodes yields an approximate solution u' for $p = 1$ to the accuracy $d(\eta) = 0.78 \times 10^{-7}$ and $d_\infty(\eta) = 0.20 \times 10^{-5}$. After further 1 885 evaluations of the determinant (9 814 in total) ACPDM yields a solution with the accuracies 10^{-10} and 0.26×10^{-8} , respectively. The duration of the run of a sequential code on a 3.16 GHz Intel Core Duo processor is 1 hr. 46 min. 24 sec. (wallclock time).

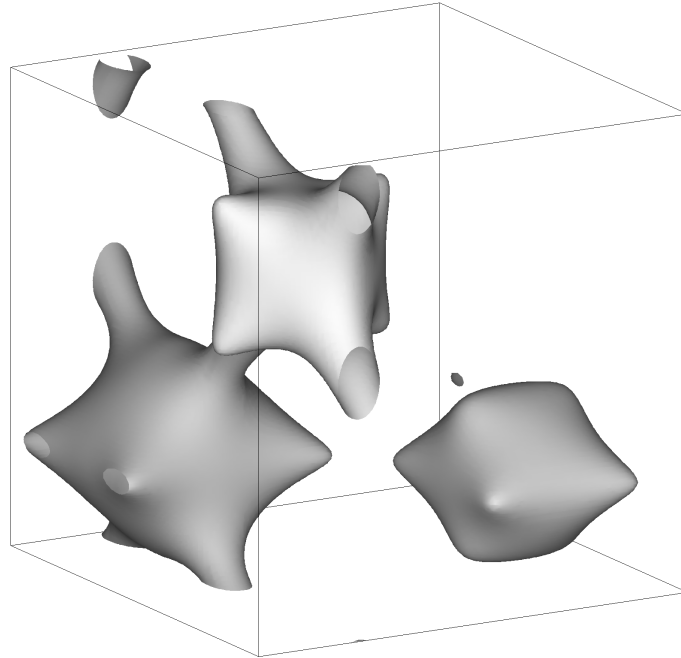


Number of evaluations of the determinant of the Hessian (vertical axis, logarithmic scale) performed by ACPDM in successive computations of solutions $\eta(p_j)$ to the gMAE to the accuracy $d(\eta, p_j) < 10^{-10}$. Horizontal axis: the index j numbering consecutive nodes p_j .



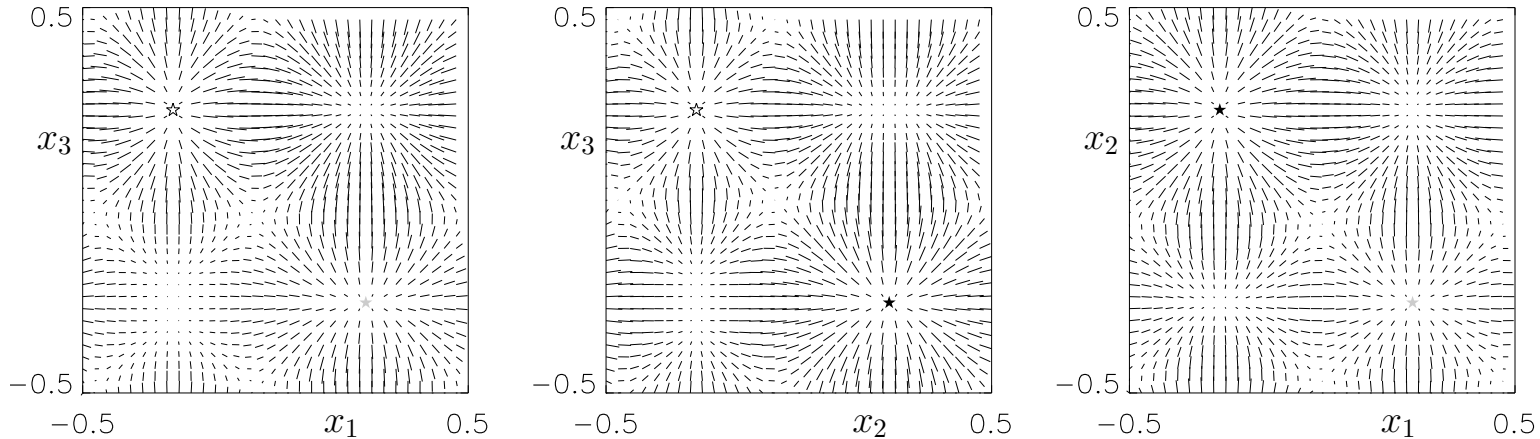
$(-0.5, -0.5, -0.5)$

Isosurfaces of the solution to the test MAE at the levels of a half and 1/8 of the maximum. The periodicity cell T^3 of u' is shown.

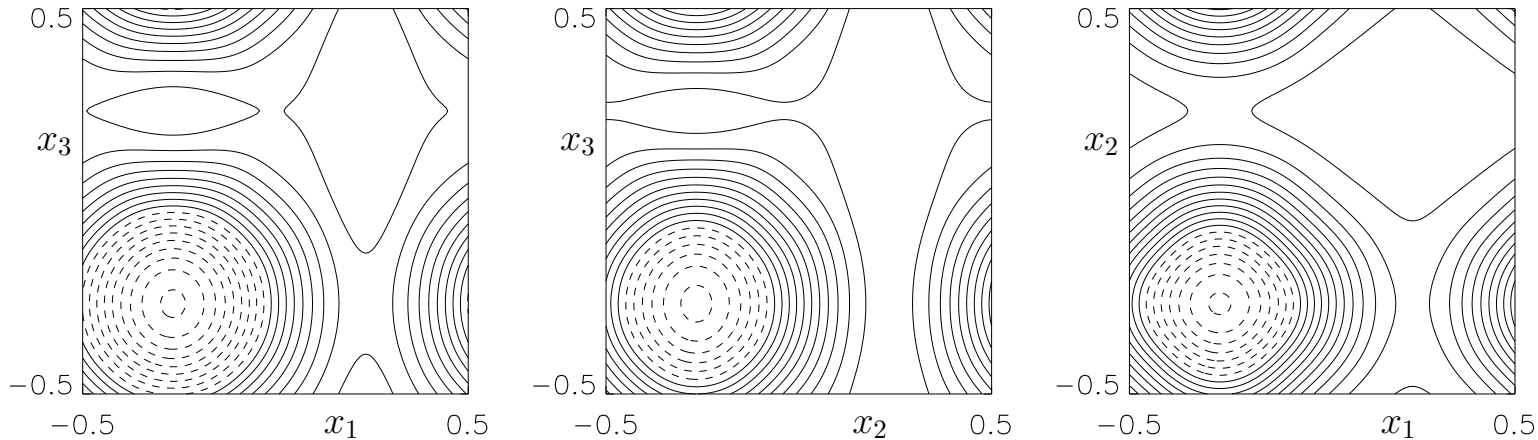


$(-0.5,-0.5,-0.5)$

Isosurfaces of $\nabla^2 u'$ for the solution to the test MAE at the level of $1/3$ of the maximum.



$\nabla u'$ for the solution to the test MAE on cross sections of the periodicity cell, parallel to coordinate planes and containing pairs of objects (left to right): $x_2 = -1/4$, $x_1 = -1/4$, $x_3 = -1/4$. (Due to the hidden symmetry of u' about each of the three planes, components of gradients normal to the planes are zero.) The labels x_i refer to the Cartesian coordinate axes, parallel to sides of the cross sections. Stars show locations of the three localised objects on the cross sections. Gray-scaling codes the masses of the objects (black, gray and white stars: the objects at $\mathbf{r}^{(g)}$, $g = 1, 2, 3$, respectively).



Isolines step 0.02 of normal components of $\nabla u'$ for the solution to the test MAE (dashed lines: negative values, solid lines: zero and positive values) on Cartesian coordinate planes (left to right) $x_2 = 0$, $x_1 = 0$, $x_3 = 0$. The labels x_i refer to the Cartesian coordinate axes, parallel to sides of the shown cross sections of T^3 .

A solver for the MAE with an everywhere positive r.h.s., AICDM

The maximum discrepancy between the 20-mode solution and the accurate one, is located at the minimum of the r.h.s., $(1/4, 1/4, 1/4)$. $\det \|u_{x_i, x_j}\| < 0$ at this point.

The (*Algorithm with Improvement of Convexity and Discrepancy Minimisation*):

a single node ($p = 1$) extension of the ACPDM, incorporating improvement of convexity of an approximate solution, which is performed whenever $d^2(\eta_K) < \beta d^2(\eta_{K'})$. K and K' are the numbers of the current iteration and of the iteration of the previous improvement of convexity, respectively; $\beta \ll 1$, we employed $\beta = 0.01$.

★ At each grid point in the physical space, compute the eigenvalues λ of $\|\nabla^{-2}(\eta_K)_{x_i x_j}\|$ (all real, since the Hessian is a symmetric matrix).

★ If all $\lambda > -1$, the approximate solution $\frac{1}{2}|\mathbf{x}|^2 + u'$ is locally convex \Rightarrow no action taken.

★ Suppose $\lambda_{\min} < -1$. The minimum eigenvalue would become -1 , if $u'_{x_i x_i}$ is increased $\forall i$ by $-1 - \lambda_{\min}$, and hence the Laplacian $\eta_K = \nabla^2 u'$ is increased by $3(-1 - \lambda_{\min})$.

\Rightarrow At a point, where $\lambda_{\min} < -1$ increase η_K by $6(-1 - \lambda_{\min})$

(using the factor 6 instead of 3, we “overimprove” η_K).

★ Repeat the procedure till all $\lambda > -1 - d(\eta_K)/2$. (The discrepancy $d(\eta'_K)$ for the “improved” approximation η'_K is allowed to exceed the initial discrepancy $d(\eta_K)$.)

We have inspected convergence of AICDM employing scalar products with weights:

$$(\mathbf{u}, \mathbf{v}) = \int_{T^3} u(\mathbf{x})v(\mathbf{x})w(\mathbf{x})d\mathbf{x}, \quad \text{where} \quad w(x; q) = \max\left(1, (\hat{f}/\langle\hat{f}\rangle)^q\right).$$

Duration of the shortest run, for $q = -1/2$, with a sequential code on the 3.16 GHz Intel Core Duo processor is 25 min. 19 sec. (a gain 4 times compared to the ACPDM).

Number of evaluations (NE) of the determinant of the Hessian performed by AICDM with the use of various weights. All runs are terminated as soon as $d(\eta, 1) < 10^{-10}$.

$d(\eta, 1) = 0.66 \times 10^{-10}$ for $q = -1$, $d(\eta, 1) = 0.95 \times 10^{-10}$ for $q = -3/4$ and $d(\eta, 1) = 1.0 \times 10^{-10}$ in all remaining cases.

q	-1	-3/4	-1/2	-1/4	0	1/4
NE	3 169	2 619	2 465	3 743	2 653	2 571
$d_\infty(\eta)$	0.09×10^{-8}	0.14×10^{-8}	0.21×10^{-8}	0.62×10^{-8}	0.41×10^{-8}	0.39×10^{-8}

q	1/2	3/4	1	5/4	3/2	7/4	2
NE	2 568	2 643	2 523	2 489	2 481	2 505	2 526
$d_\infty(\eta)$	0.37×10^{-8}	0.39×10^{-8}	0.36×10^{-8}	0.38×10^{-8}	0.39×10^{-8}	0.41×10^{-8}	0.37×10^{-8}

An enhanced version of AICDM, EAICDM

Gradual refinement of solutions with the resolution of $(16M)^3$ Fourier harmonics ($1 \leq M \leq 4$ is integer). When seeking a 64^3 -harmonics solution of the accuracy $d(\eta, 1) < 10^{-\kappa}$, the $(16M)^3$ computations are terminated when $d(\eta, 1) < 10^{-\min(\kappa, 2.5M)}$.

A further acceleration is likely to be achieved by avoiding dealiasing.

Number of evaluations (NE) of the determinant of the Hessian performed by AICDM in the course of computation of solutions of varying accuracy to the test MAE, and wallclock duration of runs (DR, seconds) by EAICDM.

$d(\eta)$	10^{-3}	10^{-4}	10^{-5}	10^{-6}
$d_\infty(\eta)$	0.64×10^{-2}	0.86×10^{-3}	1.02×10^{-3}	0.23×10^{-4}
NE	64	126	251	439
DR	3.38	4.69	11.17	42.7

$d(\eta)$	10^{-7}	10^{-8}	10^{-9}	10^{-10}
$d_\infty(\eta)$	0.28×10^{-5}	0.39×10^{-6}	0.36×10^{-7}	0.41×10^{-8}
NE	1 018	1 515	2 030	2 653
DR	81	203	435	774

Conclusion

- Three novel forms of the Monge–Ampère equation in R^N : the second-order divergence, Fourier integral and convolution forms.
- Three novel algorithms for numerical solution of the MAE with the positive r.h.s. for an odd N (the positiveness not required for ACPDM).

Open questions:

- ★ Does the gMAE always have a solution, as long as the MAE does? Does the solution of the gMAE depend analytically on the parameter p , and hence polynomial extrapolation for $p = 1$ is mathematically sensible?
- ★ Apparently the algorithms are still applicable for other regions (although the inversion of the Laplacian becomes more difficult). Do we still need the same a_m 's?
- ★ What scalar product is optimal for acceleration of convergence of ACPDM?
- ★ What is the asymptotics of solutions in the small parameter δ determining the width of the localised objects?
- ★ How does the contrast number measure numerical complexity of the MAE and, in particular, the condition number of the linearisation near the solution (for a given spatial discretisation)?
- ★ Interesting applications for our algorithms.